Cell Reports
Article

Regulation of DNA Methylation Patterns by CK2-Mediated Phosphorylation of Dnmt3a

Rachel Deplus,[1,14] Loïc Blanchon,[1,14] Arumugam Rajavelu,[2,14] Abdelhalim Boukaba,[1,14] Matthieu Defrance,[1] Judith Luciani,[1] Françoise Rothé,[3] Sarah Dedeurwaerder,[1] Hélène Denis,[1] Arie B. Brinkman,[4] Femke Simmer,[4] Fabian Müller,[7] Benjamin Bertin,[1] Maria Berdasco,[8] Pascale Putmans,[1] Emilie Calonne,[1] David W. Litchfield,[9] Yvan de Launoit,[10] Tomasz P. Jurkowski,[2] Hendrik G. Stunnenberg,[4] Christoph Bock,[5,6,7] Christos Sotiriou,[3] Mario F. Fraga,[11] Manel Esteller,[8,12,13] Albert Jeltsch,[2,*] and François Fuks[1,*]

[1]Laboratory of Cancer Epigenetics, Faculty of Medicine, Université Libre de Bruxelles, 808 route de Lennik, 1070 Brussels, Belgium
[2]Institute of Biochemistry, Stuttgart University, Pfaffenwaldring 55, 70569 Stuttgart, Germany
[3]Breast Cancer Translational Research Laboratory J.C. Heuson, Jules Bordet Institute, Université Libre de Bruxelles, 1000 Brussels, Belgium
[4]Nijmegen Centre for Molecular Life Sciences, Radboud University, 6500 HB Nijmegen, the Netherlands
[5]CeMM Research Center for Molecular Medicine of the Austrian Academy of Sciences, 1090 Vienna, Austria
[6]Department of Laboratory Medicine, Medical University of Vienna, 1090 Vienna, Austria
[7]Max Planck Institute for Informatics, 66123 Saarbrücken, Germany
[8]Cancer Epigenetics and Biology Program (PEBC), Bellvitge Biomedical Research Institute (IDIBELL), L'Hospitalet de Llobregat, Barcelona 08907, Catalonia, Spain
[9]Department of Biochemistry, Schulich School of Medicine & Dentistery, University of Western Ontario, London ON N6A 5C1, Canada
[10]UMR 8161, CNRS, Institut Pasteur de Lille, Universités de Lille 1 et 2, Institut de Biologie de Lille, 1 rue Calmette, 59021 Lille, France
[11]Centro Nacional de Biotecnología (CNB-CSIC) and Unidad de Epigenética del Cáncer, Instituto Universitario de Oncología del Principado de Asturias, 33006-Oviedo, Spain
[12]Department of Physiological Sciences II, School of Medicine, University of Barcelona, 08036 Barcelona, Catalonia, Spain
[13]Institució Catalana de Recerca i Estudis Avançats (ICREA), 08010 Barcelona, Catalonia, Spain
[14]Co-first author
*Correspondence: albert.jeltsch@ibc.uni-stuttgart.de (A.J.), ffuks@ulb.ac.be (F.F.)
http://dx.doi.org/10.1016/j.celrep.2014.06.048

SUMMARY

DNA methylation is a central epigenetic modification that is established by de novo DNA methyltransferases. The mechanisms underlying the generation of genomic methylation patterns are still poorly understood. Using mass spectrometry and a phosphospecific Dnmt3a antibody, we demonstrate that CK2 phosphorylates endogenous Dnmt3a at two key residues located near its PWWP domain, thereby downregulating the ability of Dnmt3a to methylate DNA. Genome-wide DNA methylation analysis shows that CK2 primarily modulates CpG methylation of several repeats, most notably of Alu SINEs. This modulation can be directly attributed to CK2-mediated phosphorylation of Dnmt3a. We also find that CK2-mediated phosphorylation is required for localization of Dnmt3a to heterochromatin. By revealing phosphorylation as a mode of regulation of de novo DNA methyltransferase function and by uncovering a mechanism for the regulation of methylation at repetitive elements, our results shed light on the origin of DNA methylation patterns.

INTRODUCTION

DNA methylation in mammalian somatic cells is mainly confined to cytosine bases within CpG dinucleotides. It is associated with a repressed chromatin state and inhibition of gene expression (Deaton and Bird, 2011). Methylated CpG dinucleotides are not randomly distributed throughout the genome. Rather, some genomic sequences (e.g., heterochromatic DNA) are heavily methylated, while others, such as CpG islands in the promoter regions of many genes, are usually methylation-free (Deaton and Bird, 2011). The establishment of DNA methylation patterns in mammalian cells results mainly from the action of the so-called de novo DNA methyltransferases Dnmt3a and Dnmt3b (Denis et al., 2011; Law and Jacobsen, 2010; Okano et al., 1999). Apart from some sequence specificity for residues flanking the CpG site (e.g., Handa and Jeltsch, 2005; Jurkowska et al., 2011; Lin et al., 2002), these enzymes do not appear to have any sequence specificity, so the mechanisms underlying the generation of DNA methylation patterns by Dnmts remain poorly understood. Because phosphorylation is a very important posttranslational modification that can control protein-protein interactions, enzymatic activities, and subcellular localization of proteins and has a role in many cellular processes (Johnson and Barford, 1993), we examined whether phosphorylation might regulate the function of the Dnmt3a de novo DNA methyltransferase. We focused on Dnmt3a because not much is known about PTM modification

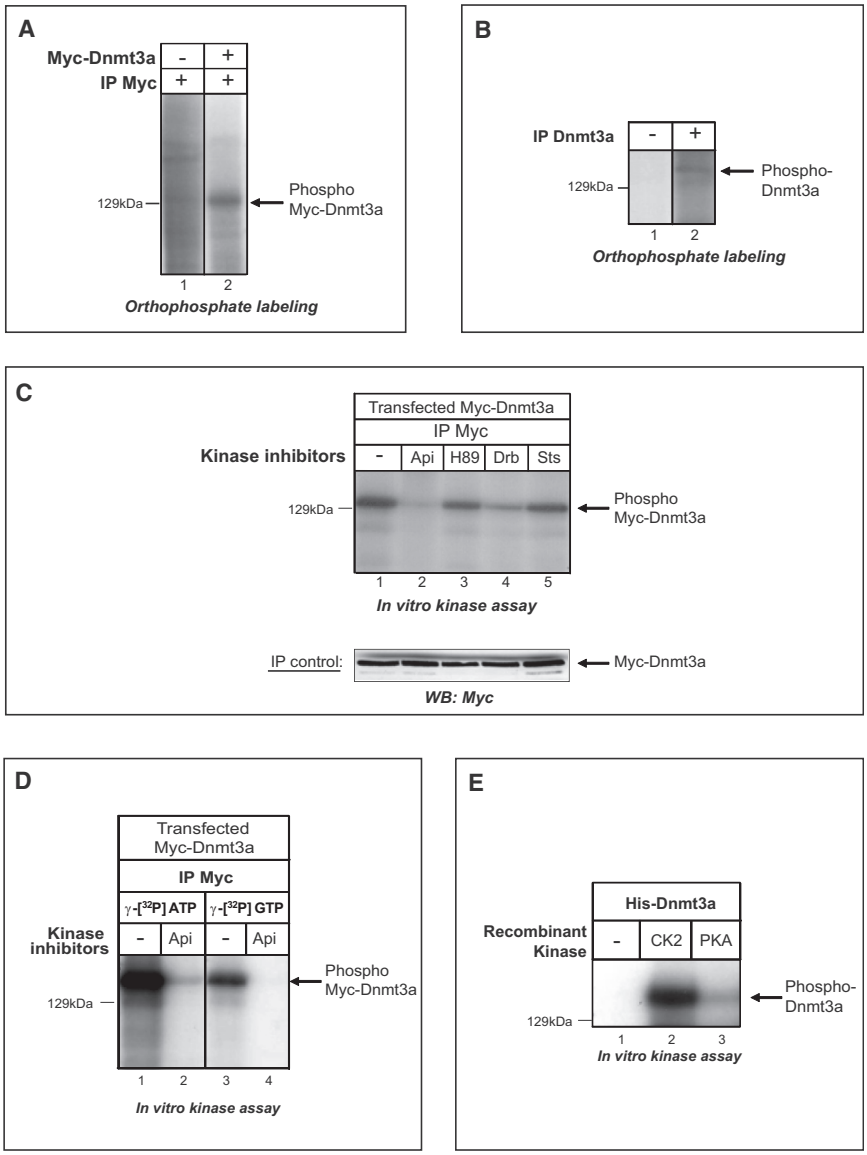

Figure 1. The De Novo DNA Methyltransferase Dnmt3a Is Phosphorylated by CK2 In Vitro and In Vivo

(A) Orthophosphate labeling of Dnmt3a-overexpressing cells. U2OS cells were transiently transfected with Myc-Dnmt3a (lane 2) or empty vector (lane 1) and incubated with ^{32}Pi for 4 hr prior to immunoprecipitation (IP) with Myc antibody. A representative experiment is shown, which was successfully repeated three times.

(B) Orthophosphate labeling of untransfected cells, followed by mock IP (lane 1) or IP with anti-Dnmt3a (lane 2). A representative experiment is shown, which was successfully repeated twice.

(C) Pharmacological inhibition of various kinases suggests that CK2 plays a major role in Dnmt3a phosphorylation. U2OS cells were transiently transfected with Myc-Dnmt3a or empty vector prior to IP with anti-Myc. Immunoprecipitated extracts were supplemented with γ^{32}P-[ATP] in the presence or absence of the indicated kinase inhibitors. Loading controls are shown in the lower panel. A representative experiment is shown, which was repeated three times.

(D) The kinase that phosphorylates Dnmt3a displays a unique feature of CK2: it can use GTP as well as ATP. Experiments were performed as in (C), with either γ^{32}P-ATP (lanes 1 and 2) or γ^{32}P-[GTP] (lanes 3 and 4). Apigenin inhibitor was used as indicated. A representative experiment is shown, which was repeated twice.

(E) CK2 phosphorylates bacterially expressed Dnmt3a. In vitro kinase assays were performed with His-Dnmt3a and recombinant CK2. Recombinant PKA was used as negative control. A representative experiment is depicted, which was repeated three times. In each panel, the vertical line indicates juxtaposition of lanes nonadjacent within the same blot/film, exposed for the same time.

of this particular Dnmt, yet there is a growing interest in better understanding its function in physiological and pathological contexts. For example, Dnmt3a has now been shown to be mutated in several cancers (Roller et al., 2013).

RESULTS

The De Novo DNA Methyltransferase Dnmt3a Is Phosphorylated by CK2 In Vitro and In Vivo

To investigate whether Dnmt3a undergoes phosphorylation, we first performed in vivo ^{32}P-orthophosphate labeling experiments after transfection of U2OS human osteosarcoma cells with a construct encoding Myc-tagged mouse Dnmt3a. After immunoprecipitation of Myc-Dnmt3a with anti-Myc and subsequent SDS-PAGE, we observed a band of overexpressed Dnmt3a having incorporated ^{32}P, whereas mock-transfected cells showed no corresponding band (Figure 1A). Similar experiments with ^{32}P-labeled nontransfected U2OS cells revealed, after immunoprecipitation of endogenous Dnmt3a, that this human enzyme was also phosphorylated (Figure 1B, lane 2). As a negative control, a mock immunoprecipitation was carried out with the same labeled extracts (Figure 1B, lane 1). Dnmt3a is thus posttranslationally modified by phosphorylation in vivo.

Next, to identify the kinase(s) responsible for the observed Dnmt3a phosphorylation, we purified Myc-tagged Dnmt3a from U2OS cells by immunoprecipitation and subjected it to in vitro kinase assays performed with cell extracts supplemented or not with various kinase inhibitors. In agreement with the data presented in Figures 1A and 1B, this assay revealed the presence of phosphorylated Dnmt3a (Figure 1C, lane 1). Dnmt3a phosphorylation was unaffected by several kinase inhibitors, such as H89 and staurosporine (Figure 1C, lanes 3 and 5), known to primarily inhibit protein kinase A (PKA) and protein kinase C (PKC), respectively. In contrast, two potent inhibitors of CK2

activity, apigenin and Drb, caused a robust decrease in Dnmt3a phosphorylation (Figure 1C, lanes 2 and 4). Dnmt3a protein levels were unaffected by inhibitor treatment (Figure 1C, lower panel). This suggests that the ubiquitous serine/threonine protein kinase CK2 (St-Denis and Litchfield, 2009) plays a major role in Dnmt3a phosphorylation.

As kinase inhibitors often affect the activity of more than one kinase, we performed additional sets of experiments to further test this conclusion. First, we exploited a feature unique to CK2 among kinases: its ability to use GTP as well as ATP as a phosphate source (Mazzorana et al., 2008). In vitro kinase assays similar to those shown in Figure 1C revealed phosphorylation of Dnmt3a in the presence of γ-[^{32}P] GTP, albeit to a lower level than when labeled ATP was used (Figure 1D). Second, to test directly whether Dnmt3a can be a substrate of CK2, we performed an in vitro kinase reaction using bacterially expressed histidine-tagged Dnmt3a and recombinant CK2 in the presence of labeled ATP. After SDS-PAGE and autoradiography, Dnmt3a appeared to be efficiently phosphorylated by CK2 (Figure 1E, lane 2). In a negative control where recombinant PKA was included instead of CK2 (Figure 1E, lane 3), Dnmt3a remained unlabeled.

Dnmt3a Is Phosphorylated by CK2 at S386 and S389

Having established Dnmt3a is a bona fide substrate for CK2, we set out to identify the target residues of CK2. In silico screening for CK2 consensus sites S/TxxD/E or S/TxD/E (Allende and Allende, 1995) revealed several potential sites in two regions of Dnmt3a, one encompassing its conserved Pro-Trp-Trp-Pro motif (PWWP) domain (also called the "extended PWWP" below) and one comprising its C-terminal catalytic domain. In vitro kinase assays using recombinant CK2 revealed efficient phosphorylation of a Dnmt3a fragment spanning residues 279–420, overlapping with the PWWP domain (Figure 2A, lane 3). In contrast, the catalytic and ATRX-Dnmt3-Dnmt3L (ADD) domains of Dnmt3a (Figure 2A, lanes 2 and 7, respectively) were not appreciably phosphorylated. The extended PWWP region contains two potential CK2 sites, at serines 386 and 389, which are conserved among all Dnmt3a homologs (Figure 2C and Figure S1C). A CK2 kinase assay using variants where S386, S389, or both were replaced with A (so that these sites could no longer be phosphorylated) showed that each single mutation decreased phosphorylation weakly and the presence of both mutations almost completely abolished phosphorylation (Figure 2A, lanes 4, 5, and 6). Consistently with the above data, replacement of residues S386 and S389 with E (mimicking the phosphorylated state) abolished phosphorylation by CK2 (Figure 2B, lane 4). (One should note that the higher phosphorylation observed with the S389E single mutant [Figure 2B, lane 3] may be related to the fact that the peptide motif more closely matches the CK2 consensus target motif after the serine-to-glutamic acid mutation.) To provide additional evidence, mass spectrometry analysis was also performed with the purified extended PWWP domain after the in vitro CK2 kinase assay, gel purification, and chyomotryptic digestion. As shown in Figure 2D (and Figures S1A and S1B), a peptide containing both serine residues in phosphorylated form was identified. The structure of the Dnmt3a PWWP domain shows that the loop containing both serine residues is not ordered but exposed at the surface of the domain, indicating that it is accessible to CK2 (Figure S1C, lower part).

Next, with an antibody raised against S390- and/or S393-phosphorylated human Dnmt3a (these residues correspond to mouse residues S386 and S389; cf. Figure 2C), we demonstrated that endogenous Dnmt3a is phosphorylated by CK2 in vivo. As shown in Figure 2E, the antibody recognized a single band (lane 1), which was abolished in the presence of the singly or doubly phosphorylated peptide used for immunization (lanes 2–4), but not in the presence of its unphosphorylated equivalent (lane 5).

Lastly, to obtain further in vivo data on CK2-mediated Dnmt3a phosphorylation, we used RNAi to knock down CK2α in U2OS cells (Figure S2). By western blotting with the antibody against phospho-Dnmt3a, we observed a strong reduction of Dnmt3a phosphorylation in U2OS cells depleted of CK2 (Figure 2F).

Altogether, these data identify two serines of Dnmt3a as targets of CK2-mediated phosphorylation.

CK2 Negatively Regulates the Ability of Dnmt3a to Methylate DNA and Decreases the Overall Genomic Level of 5-Methylcytosine

We next evaluated the functional consequences of CK2-mediated Dnmt3a phosphorylation. Since the primary function of mammalian Dnmt3a is to methylate DNA, we investigated whether phosphorylation of Dnmt3a by CK2 might influence its DNA methyltransferase activity. For this we initially used DNA methyltransferase assays measuring the transfer of tritiated methyl groups from S-adenosyl-L-[methyl-^{3}H]methionine to a synthetic oligonucleotide substrate (Jurkowska et al., 2008). A recombinant Dnmt3a2/Dnmt3L complex was used to get higher enzyme activity (Dnmt3L was not phosphorylated by CK2; data not shown); Dnmt3a2 is a catalytically active Dnmt3a isoform (Chen et al., 2002). As depicted in Figure 3A, using DNA methyltransferase (DNMT) assays with recombinant Dnmt3, we found the DNA methyltransferase activity of the Dnmt3a2/Dnmt3L complex to be significantly reduced in the presence of recombinant CK2. Similar results were obtained in DNMT assays with lysate from transfected cells (Figure 3B). In these experiments, Dnmt3a was overexpressed in U2OS cells with or without CK2 wild-type (WT) or a catalytically inactive mutant (Penner et al., 1997). As shown in Figure 3B, Dnmt3a overexpression in U2OS cells led to increased DNMT activity as compared to mock-transfected cells (lanes 1 and 2). When exogenous Dnmt3a was produced together with CK2, the DNMT activity was reduced to the level detected in mock-transfected cells (Figure 3B, lanes 1 and 4). No such effect was observed when Dnmt3a was overexpressed together with the the catalytically inactive CK2 mutant or with PKA (Figure 3B, lanes 5 and 6). We also performed DNMT assays using phosphomimetic Dnmt3a mutants. As shown in Figure 3C, DNA methyltransferase activity was slightly lower with either single phosphomimetic mutant (S386E or S389E) than with the wild-type, and the S386E/S389E double mutant showed even lower DNMT activity. Additional controls showed that inactivated CK2 did not repress Dnmt3a and Dnmt3a mutants were not affected by CK2 either (Figure S3).

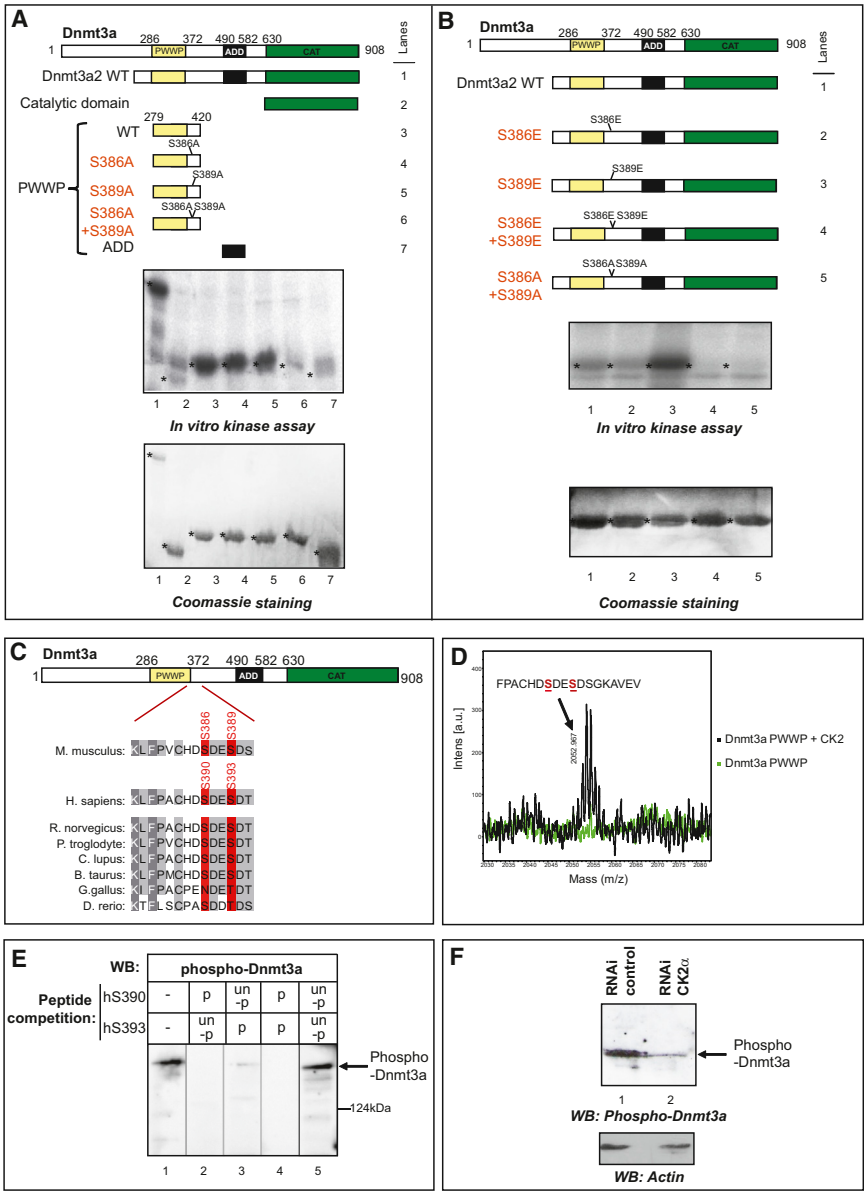

Figure 2. Dnmt3a Is Phosphorylated by CK2 at S386 and S389

(A and B) His fusions of Dnmt3a2. The indicated fusions were tested in in vitro kinase assays with recombinant CK2. The middle panel shows autoradiograms of in vitro kinase assays performed with the indicated His-Dnmt3a fusion proteins. The lower panel shows Coomassie staining as loading control. In each panel, a representative experiment is shown, which was repeated three times.

(C) Residues S386 and S389 (red), phosphorylated in mouse Dnmt3a, are conserved among its homologs from all species (e.g., S390/S393 in humans).

(D) Mass spectrometry analysis of Dnmt3a after phosphorylation by CK2. At a sequence coverage of 72.4% and an intensity coverage of 38.2%, one peptide is detected (2,052.96 Da; arrow), corresponding to a doubly phosphorylated fragment (FPACHDSDESDSGKAVEV, theoretical mass: 2,052.73 Da) containing S386 and S389 (in red, underlined). This peak was not detected without prior phosphorylation (in green). Numbers represent the masses of the substrate and product peptides. The MALDI experiments were carried out twice.

(E) Phosphorylation of endogenous human Dnmt3a by CK2 in vivo. Lysates from untransfected U2OS cells were subjected to western blotting with phospho (S390/393) human Dnmt3a antibody in the absence and presence of the indicated phosphorylated (p) or unphosphorylated (un-p) peptide. A representative experiment is shown, which was successfully repeated three times. The vertical line indicates juxtaposition of lanes within the same blot, exposed for the same time.

(F) Human Dnmt3a phosphorylation is decreased in CK2α-depleted U2OS cells. The western blot with phospho (S390/393) human Dnmt3a antibody shows reduction of endogenous DNMT3A phosphorylation in the presence of an RNAi targeting CK2α (lane 2), as compared to an RNAi control (lane 1). Actin levels were checked to confirm that equal amounts of extract were used.

Having established that CK2-mediated phosphorylation of Dnmt3a reduces its DNA methyltransferase activity in vitro, we examined the effect of CK2 on global DNA methylation in vivo. To this end, we used a previously characterized inducible Tet-Off U2OS cell line, where the levels of CK2α catalytic subunits can be manipulated with tetracycline (Tc) (Vilk et al., 1999). In the Tet-Off cell line, CK2α expression is at the endogenous level in the absence of tetracycline but CK2α is strongly induced in the presence of tetracycline (Vilk et al., 1999) (data not shown). In this cell line, we measured the total 5-methylcytosine (5mC) content by high-performance capillary electrophoresis (HPCE) (Fraga et al., 2005). As shown in Figure 3D (lanes 1 and 2), increased expression of CK2α WT (in the absence of Tc) resulted in a significantly decreased genomic 5mC content. As controls, we also used a similar U2OS Tet-Off cell line, this time stably expressing a catalytically inactive CK2α. As depicted in Figure 3D (compare lanes 3 and 4), induced expression of catalytically inactive CK2α did not decrease the genomic 5mC content.

Next, we have performed HPCE experiments in U2OS WT cells or cells depleted of CK2. As depicted in Figure 3E, we found that an RNAi targeting CK2 led to a significant increase in total CpG methylation (Figure 3E). These data, obtained by manipulating endogenous CK2, further extend and confirm the impact of CK2 on the overall genomic level of 5-methylcytosine.

CK2 Influences Genome-wide CpG Methylation

To investigate the influence of CK2 on genome-wide DNA methylation, we used the methylated DNA capture-sequencing (MethylCap-seq) method, in which methylated genomic DNA is

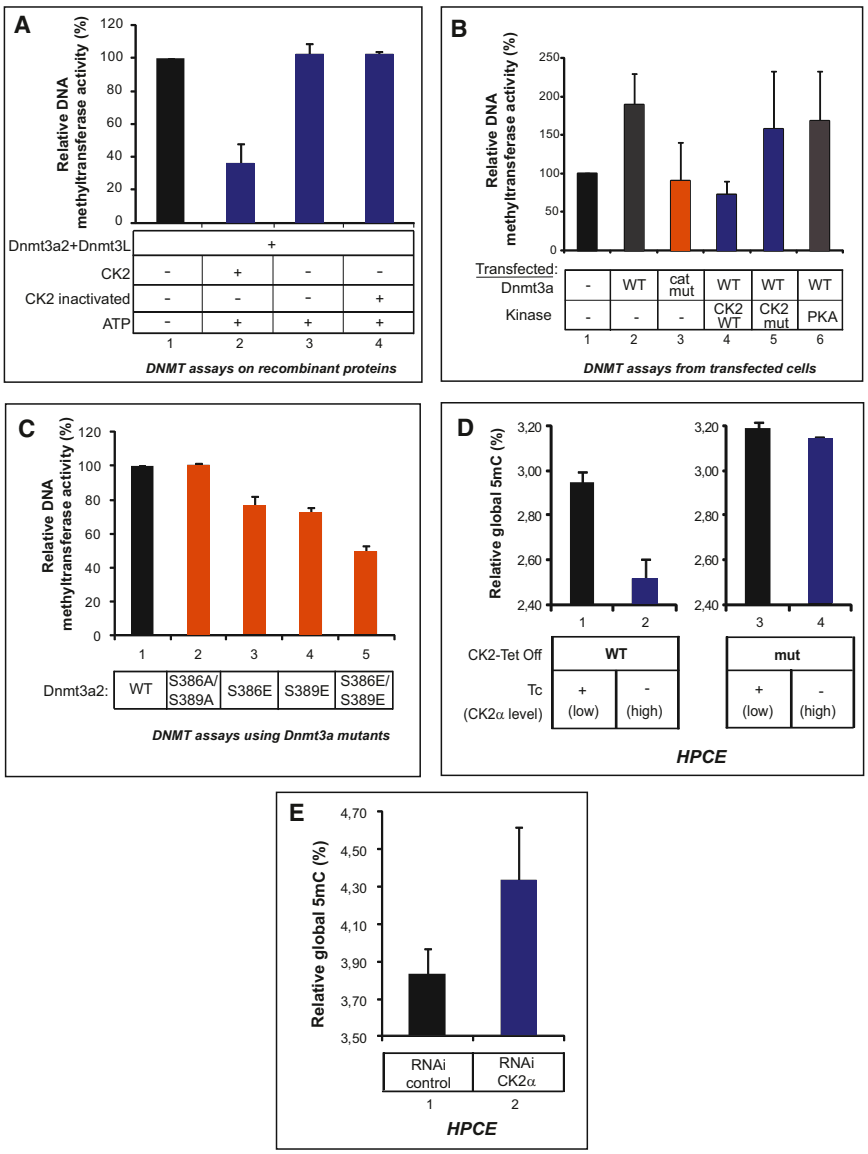

Figure 3. CK2 Negatively Regulates the Ability of Dnmt3a to Methylate DNA and Decreases the Overall Genomic Level of 5-Methylcytosine

(A) CK2 reduces Dnmt3a methyltransferase activity. Following phosphorylation of Dnmt3a2 by CK2 as indicated, DNA methyltransferase activity was assayed by incubating an oligonucleotide substrate with S-adenosyl-L-[methyl-^{3}H]-methionine and measuring incorporation of the radiolabeled methyl group into the substrate. The recombinant Dnmt3a2+Dnmt3L complex was used to get higher enzyme activity. Error bars represent SD of biological duplicates.

(B) CK2 reduces DNMT activity in transfected cells. U2OS cells were transfected so as to express Dnmt3a and/or CK2 WT or a catalytically inactive mutant (Penner et al., 1997) thereof. In vitro kinase assays followed by DNMT assays were then performed. PKA, used as a negative control, did not alter DNMT activity. Error bars represent SD of biological duplicates.

(C) Use of a phosphomimetic Dnmt3a mutant results in decreased DNMT activity. Experiments were done as in (A) with the indicated recombinant Dnmt3a2 protein. Error bars represent SD of biological duplicates.

(D) CK2 decreases overall genomic DNA methylation. HPCE (Fraga et al., 2005) was performed on extracts of Tet-Off CK2 cells to measure the total 5mC content. Error bars represent SD of duplicate experiments.

(E) CK2-depleted cells show an increased global DNA methylation level. Total genomic 5mC was measured by HPCE on DNA from RNAi control and CK2 RNAi U2Os cells. Error bars represent SD of triplicate experiments.

captured by affinity purification with a methyl-binding domain (MBD) protein and subjected to high-throughput sequencing (Bock et al., 2010; Martens et al., 2010). First, we focused on the nonrepetitive portion of the genome. As shown in Figure 4A, CK2-depleted cells and control cells showed the same MethylCap-seq profile. Likewise, when CpG methylation was quantified with Illumina's Infinium Methylation Assay (Bibikova et al., 2009), no difference in DNA methylation was detected between cells treated with control or CK2α RNAi (Figure S4).

Next, we performed MethylCap-seq experiments performed on control and CK2α-depleted cells to assess the methylation of repetitive DNA. For this, we used a set of prototypic repeat sequences to identify differentially methylated repetitive elements (see Experimental Procedures for details). This was of particular interest, as genome-wide studies on DNA methylation in repetitive regions are scarce to date. In many repetitive elements, we found significant differences in DNA methylation between CK2α-knockdown and control cells. As shown in Figures 4B–4D (see also Figures S5A and S5B for a detailed view of the affected repeats), we observed both significant hypermethylation (elements in red in Figures 4B and 4C) and significant hypomethylation (elements in green). Note that dot size reflects the element's statistical significance and dot color indicates the repeat type (e.g., short interspersed nuclear element [SINE], long interspersed nuclear element [LINE]) of the element (see also Experimental Procedures). We then investigated how specific types of differentially methylated elements contribute to the overall differential methylation pattern (Figure 4C and 4D). As compared to control cells, CK2-knockdown cells mainly showed hypermethylated elements, mostly of the SINE type (e. g. Alu), but hypomethylated elements were also identified, most of them being LINE, long terminal repeat (LTR), or satellite elements (Figures 4D and S5C). Lastly, using the MethylCap-seq data, we investigated repeat class location, with a focus on methylation changes in LINEs and SINEs according to their genomic location. We found SINEs and LINEs displaying differential methylation to be located both in intergenic regions and within gene bodies (Figure S5C).

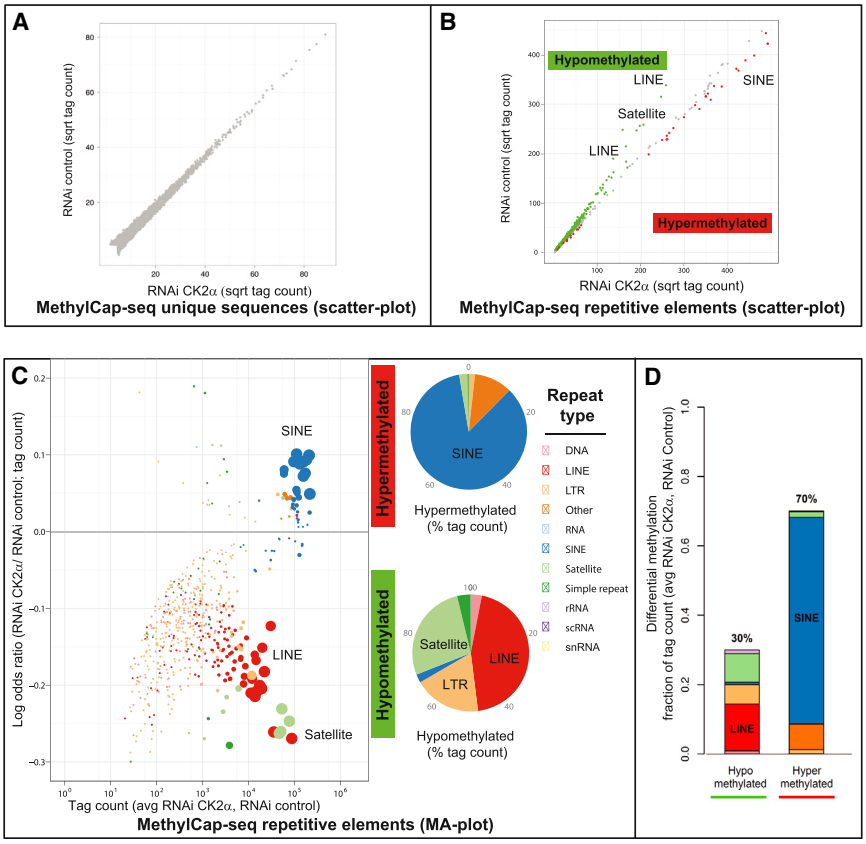

Figure 4. Genome-wide CpG Methylation Analysis

(A) Depletion of cellular CK2α does not affect CpG methylation of unique sequences. GST-MBD pull-down (MethylCap) followed by deep sequencing was performed in control and CK2α-knockdown cells to assess the effect of CK2α knockdown on global DNA methylation pattern. Sequenced reads were uniquely mapped to the human genome and peaks were called (see Experimental Procedures for details). The pairwise scatterplot of the number of tags (mapped reads) for the RNAi CK2α sample versus the number of tags for the RNAi control sample for the detected peaks reveals no significant differentially methylated region.

(B) Control and CK2α-depleted cells show significant differential methylation of certain repeats. GST-MBD pull-down (MethylCap) followed by deep sequencing was performed on control and CK2α-knockdown cells to assess global changes in DNA methylation. Sequenced reads were mapped to a set of prototypic repeats obtained from the RepBase Update database (see Figure S5B and Experimental Procedures for details). The pairwise scatterplot of the number of tags (mapped reads) for the RNAi CK2α sample versus the number of tags for the RNAi control sample for the prototypic sequences shows both hypermethylated repeats (in red) and hypomethylated repeats (in green) in knockdown versus control cells.

(C) Most of the hypermethylated elements are of the SINE repeat type, while the hypomethylated elements belong to the LINE, LTR, and satellite types. On the left, the MA plot shows the distribution of hypo- and hypermethylated elements (log odds ratio of the tag count in the RNAi CK2α sample versus the tag count in the control sample) divided by the average log tag count. The upper part shows the hypermethylated elements (log odds ratio > 0) in the RNAi CK2α sample, while the lower part shows hypomethylated elements (log odds ratio < 0). Dot size reflects the statistical significance and the color indicates the repeat type (e. g. SINE, LINE) to which each element belongs. On the right, the pie charts show the distribution of tags (% of tags) according to the repeat type for both the hyper- and hypomethylated elements (see Experimental Procedures for details).

(D) Differentially methylated repetitive elements show a large proportion of hypermethylation (70% of tags) and a lower proportion of hypomethylation (30% of tags) in RNAi-CK2α versus RNAi control cells (upper part, bar plots). For both hyper- and hypomethylated elements, the distribution of tags (% of tags) corresponding to each type of repetitive element are shown as a stacked bar plot (see Experimental Procedures for details). Hypermethylated elements are mostly represented by SINE elements and hypomethylated elements by LINEs, LTRs, and satellites. Hyper- and hypomethylation were assessed by means of Fisher's exact statistical test with multiple correction based on Storey's q value. Elements with a q value < 0.05 and an absolute odds ratio > 1.1 were considered differentially methylated (see Experimental Procedures for details of analyses).

Regulation of Alu SINEs DNA Methylation Is Linked to CK2-Mediated Dnmt3a Phosphorylation

Next, to zoom in on SINEs, we performed bisulfite sequencing on Alu elements. We focused on these elements because they displayed the biggest changes in methylation upon CK2 knockdown (cf. Figure 4D). First, we used CK2α-depleted U2OS cells (i.e. e., the same cells as for the methylated DNA-capture experiments). As shown in Figure 5A, we observed increased methylation at these repeats after CK2 knockdown, thus confirming our MethylCap-seq data. Next, we used cells overexpressing CK2 and observed reduced Alu methylation (Figure 5B).

Lastly, we assessed whether the regulation of DNA methylation by CK2 might be directly attributable to Dnmt3a phosphorylation. For this, we transfected human embryonic kidney 293T (HEK293T) cells with expression constructs encoding either Dnmt3a WT, a Dnmt3a variant with mutated phosphorylation sites (S386A+S389A), or a phosphomimetic mutant (S386E+S389E). This was followed by bisulfite sequencing of Alu/SINE repeats. As shown in Figure 5C, cells expressing the nonphosphorylatable double-A Dnmt3a variant (S386A/S389A) showed increased methylation at Alu repeats as compared to untransfected cells. In contrast, cells transfected with the phosphomimetic double-E mutant (S386E/S8389E) showed the same degree of methylation at Alu repeats as untransfected cells. Thus, the above methylation data with Alu SINE elements very well agree with our findings of methylation changes at the global level. In addition, when taken together, these data indicate that CK2-mediated regulation of DNA methylation is directly linked to Dnmt3a phosphorylation by CK2, although CK2 has many protein targets in the cell (Allende and Allende, 1995).

CK2-Mediated Phosphorylation of Dnmt3a Favors Its Heterochromatin Localization

Previous immunofluorescence studies on mouse NIH 3T3 cells have shown that Dnmt3a localizes essentially to heterochromatin, this localization being dependent on a Dnmt3a region

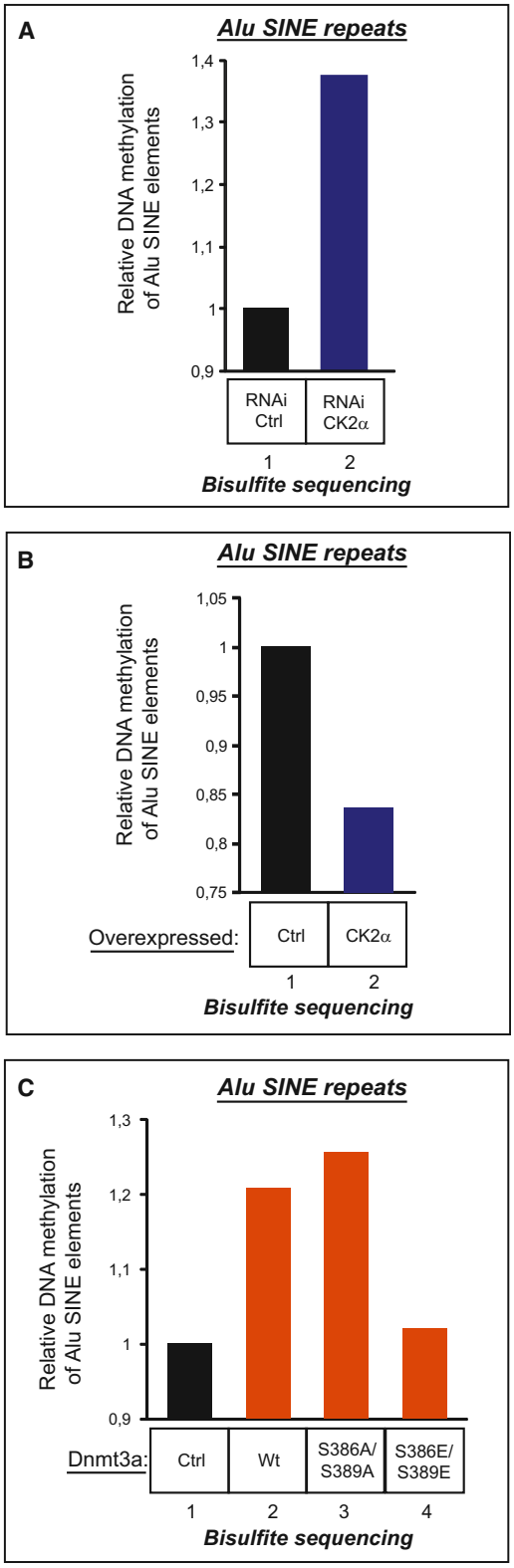

Figure 5. CK2-Mediated Dnmt3a Phosphorylation Controls Alu/SINE DNA Methylation

(A) Bisulfite sequencing shows increased methylation at Alu/SINE repeats after CK2 knockdown in U2OS cells. Genomic DNA from cells expressing a control RNAi or CK2α RNAi were essayed for DNA methylation of Alu repeats after bisulfite conversion.

(B) Reduction of DNA methylation at Alu/SINE repeats in CK2-overexpressing cells. DNA was isolated from U2OS cells after CK2 overexpression and from control cells and the level of Alu/SINE repeat DNA methylation was measured after bisulfite conversion.

(C) Impact of Dnmt3a phospho mutants on the methylation of Alu/SINE repeats. Cells were transfected with a construct encoding Dnmt3a WT, a Dnmt3a mutant lacking phosphorylation sites (S386A+S389A), or a phosphomimetic mutant (S386E+S389E). Bisulfite sequencing was then performed to evaluate methylation at Alu/SINEs. All Alu DNA methylation levels are reported relative to methylation observed in the presence of the control RNAi in the corresponding experiments.

encompassing the extended PWWP portion (Chen et al., 2004; Dhayalan et al., 2010; Ge et al., 2004). We thus wondered whether CK2-mediated phosphorylation of Dnmt3a at S386 and S389 next to its PWWP domain (cf. Figures 1 and 2) might modulate its localization to heterochromatin. When NIH 3T3 cells expressing enhanced yellow fluorescent protein (EYFP)-fused Dnmt3a WT were examined by fluorescence microscopy, we detected Dnmt3a WT in large spots corresponding to DAPI-stained heterochromatin as reported earlier (Chen et al., 2004; Dhayalan et al., 2010; Ge et al., 2004) (Figures 6A and S6F). A similar heterochromatic localization was observed with the phosphomimetic double-E Dnmt3a mutant (S386E/S8389E) (Figures 6A, S6B, and S6F). In contrast, the double-A Dnmt3a mutant (S386A/S389A) showed a diffuse nuclear staining pattern excluding heterochromatin and compatible with a spread into euchromatin (Figures 6A and S6A). To further relate these observations to CK2-mediated phosphorylation of Dnmt3a, we performed immunofluorescence experiments as before, this time in the presence or absence of the CK2 inhibitor 4,5,6,7-tetrabromobenzotriazole (TBB). When applied to cells expressing Dnmt3a WT, TBB treatment led to a partial loss of its heterochromatic spot localization in over 60% of the cells, but when the treatment was applied to cells expressing the S386E/S389E mutant protein, the subnuclear localization remained unchanged (Figures 6B and S6C–S6E and data not shown).

To see if mutating the conserved phosphorylation sites might alter the localization of Dnmt3a in human cells also, we repeated in human cells our immunofluorescence experiment (cf. Figure 6). In agreement with the mouse data, we found that phosphorylation of Dnmt3a by CK2 controls subnuclear partitioning of Dnmt3a from the heterochromatic to the euchromatic portion of the nucleus (Figure S7), as indicated by a transition from a granular localization pattern for wild-type Dnmt3a and the phosphomimetic mutant (S386E+S389E) to homogeneous subnuclear staining of the nonphosphorylatable mutant (S386A+S389A).

Together, these data strongly suggest that phosphorylation of Dnmt3a by CK2 controls the subnuclear distribution of Dnmt3a between the heterochromatic and the euchromatic compartments of the genome.

DISCUSSION

The origin of DNA methylation patterns is a longstanding mystery, and how de novo DNA methyltransferases are preferentially

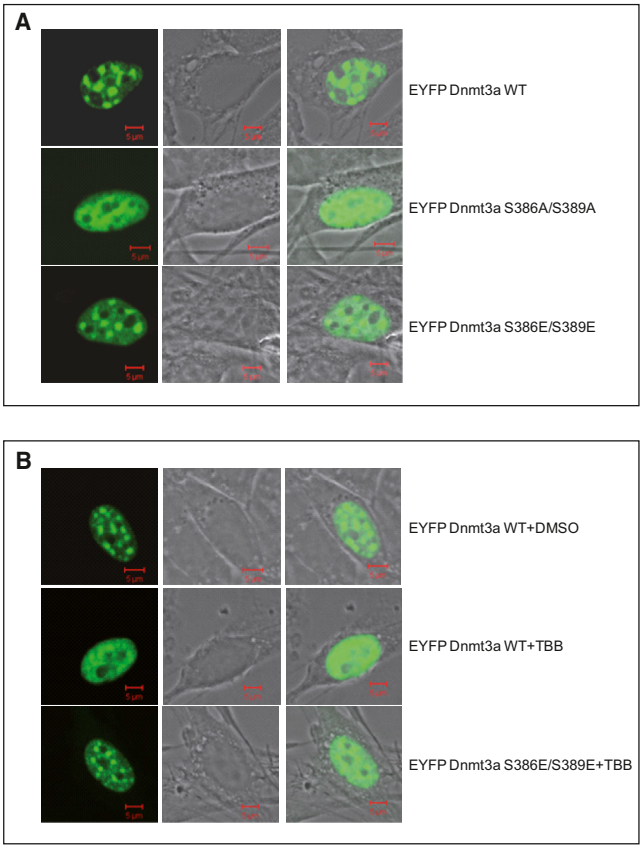

Figure 6. CK2-Mediated Phosphorylation of Dnmt3a Favors Its Heterochromatin Localization

(A) The phosphomimetic double-E Dnmt3a mutant localizes to heterochromatin, whereas the double-A Dnmt3a mutant shows spreading into the euchromatin. Dnmt3a protein localization was determined by fluorescence microscopy in NIH 3T3 cells transiently expressing the indicated Dnmt3a–EYFP. Dnmt3a WT was detected as previously reported (Chen et al., 2004; Dhayalan et al., 2010) in large spots corresponding to heterochromatin.

(B) Inhibition of CK2 by TBB results in partial loss of the heterochromatic localization of Dnmt3a WT. Immunofluorescence experiments similar to those depicted in (A) were performed in the presence or absence of the CK2 inhibitor TBB. In contrast to its effect on Dnmt3a WT, TBB did not affect the localization of the S386E/S389E mutant protein. The localization experiments were done three times. The image shows examples of individual cells.

targeted to specific regions of the genome is still poorly understood. Here, we provide evidence that DNA methylation patterns are regulated by phosphorylation of the Dnmt3a de novo DNA methyltransferase. Notably, we reveal a mechanism for the regulation of DNA methylation at repetitive elements.

Several chromatin-based mechanisms have been proposed to explain how DNA methyltransferases might find their targets in the genome (Denis et al., 2011). Our discovery that CK2-mediated Dnmt3a phosphorylation affects CpG methylation may relate to these mechanisms. The two key residues identified as important for Dnmt3a enzymatic activity and localization, S386 and S389, are situated within a region encompassing the PWWP domain, known to be involved in targeting Dnmt3a to heterochromatic sequences (Chen et al., 2004; Dhayalan et al., 2010; Ge et al., 2004). This suggests an interesting possibility: that phosphorylation of the extended PWWP domain might modulate the ability of Dnmt3a to interact with one or more components of the histone-modification and chromatin-remodeling systems (e.g., the SUV39H H3K9 enzymes [Lehnertz et al., 2003] or LSH [Huang et al., 2004]), involved in establishing DNA methylation at heterochromatin.

While our analyses of global methylation by HPCE point to a CK2-mediated decrease in methylation, genome-wide mapping of DNA methylation (by MethylCap-Seq) indicates a more complicated response. CK2 knockdown led to a methylation increase affecting 70% of the differentially methylated tags, mainly at SINE elements. In addition, a decrease in methylation was observed at a smaller number of sites (e.g., at LINEs and satellites). These data are consistent, because SINE elements contain more than one-third of the total CpGs (more than any other repeats) and account for more than one-quarter of the total CpG methylation (again well above other repeats) (e.g., (Cordaux and Batzer, 2009; Lander, 2011; Rollins et al., 2006). Furthermore, our MethylCap-seq data show that a greater number of SINE elements than LINE/LTR/satellite repeats display changes in methylation after CK2 knockdown (Figures 4C and 4D). All in all, these observations strongly suggest that the CK2-mediated reduction in global DNA methylation (as seen by HPCE; Figures 3D and 3E) results mainly from the decrease in methylation of the overrepresented SINE CpGs (as seen by MethylCap-seq; Figures 4B–4D).

Our findings suggesting that CK2-mediated phosphorylation plays an important role both in guiding Dnmt3a to specific portions of the genome and in controlling DNA methylation at certain repeats may shed light on the compartmentalization of DNA methylation in the genome. We show that phosphorylation of Dnmt3a not only reduces its activity but also reinforces its binding to heterochromatin. Both of these effects reduce its action on euchromatic targets, as exemplified by the observed hypermethylation at SINEs. Interestingly, this dual mode of regulation has recently been reported for Dnmt3L as well. Since Dnmt3L increases the activity and euchromatic localization of Dnmt3a, it is reasonable to think that this action may counteract the control of Dnmt3a by CK2. Thus, the combined regulation of activity and localization seems to be a general phenomenon, at least for Dnmt3a. On the basis of our data, we propose that the pool of Dnmt3a available for euchromatin-associated processes is kept low by CK2-mediated phosphorylation, which targets the enzyme to the heterochromatin and reduces its activity (see Figure 7 for a summary of our data).

Is the regulation of DNA methylation by CK2-mediated phosphorylation of Dnmt3a conserved between mice and humans? Three facts suggest that it is: (1) both mouse and human Dnmt3a are observed to be phosphorylated by CK2; (2) the region surrounding the Dnmt3a phosphorylation sites displays very strong conservation between mice and humans; and (3) phosphorylation of Dnmt3a by CK2 controls the subnuclear partitioning of Dnmt3a in both mouse and human cells.

Lastly, our results might also have important consequences for human disease. The constitutively active CK2 kinase is tightly regulated in normal cells. Previous studies have evidenced increased CK2 expression in cancers (Trembley et al., 2009) as well as decreased Alu SINE methylation (Bae et al., 2012; Xie

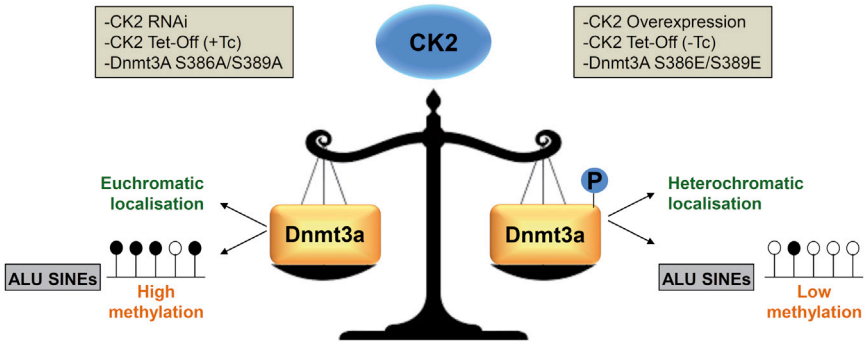

Figure 7. Summary of Results

Left: In CK2-overexpressing cells or in the phosphomimetic Dnmt3a mutant, lower Alu/SINE methylation is observed and Dnmt3a is found essentially located in the heterochromatin. Right: Conversely, in cells with downregulated CK2 or harboring the nonphosphorylatable Dnmt3a mutant, higher Alu/SINE methylation is detected and Dnmt3a is more localized to the euchromatin.

et al., 2010). The molecular basis of these observations remains largely unknown. Our bisulfite sequencing data reveal that Alu repeats show decreased methylation upon CK2 overexpression and in the phosphomimetic Dnmt3a mutant (S386E+S389E). While speculative at this stage, it is conceivable that higher CK2 levels, by leading to increased Dnmt3a phosphorylation, might be related to the reported reduced methylation of some Alu repeats in cancers. Future work will be needed to address this exciting possibility. Further studies may also be worth pursuing to assess whether CK2-mediated regulation of CpG methylation is operational also at non-CG methylation sites. Since previous reports show that non-CG methylation exists essentially in embryonic stem cells and the brain (Lister et al., 2009), it will be interesting to study the effect of CK2 on non-CpG methylation in these cells in subsequent studies.

In conclusion, our findings shed light on how posttranslational modifications might fine-tune the function of de novo DNA methyltransferases. They reveal an important mode of regulation that contributes to shaping the CpG methylation ground within the genome.

EXPERIMENTAL PROCEDURES

Cell Culture and Transfections

U2OS and NIH 3T3 cells were maintained in Dulbecco's modified Eagle's medium (GIBCO BRL) supplemented with 10% fetal bovine serum and grown at 37°C under 5% CO_2. Inducible CK2 Tet-Off U2OS cells were maintained as already described (Vilk et al., 1999, 2001). U2OS cells (HTB-96) were purchased from the ATCC and NIH 3T3 cells (ACC-59) from the German DSZM. All cells were regularly tested for mycoplasma contamination. Transient transfections were performed as described previously (Deplus et al., 2013). The vectors pcDNA3.1-myc-Dnmt3a and pcDNA3.1-EYFP-Dnmt3a have been described (Dhayalan et al., 2010; Viré et al., 2006). The vectors pcDNA3.1-EYFP-Dnmt3a-S386E/S389E and pcDNA3.1-EYFP-Dnmt3a-S386A/S389A were derived from pcDNA3.1-EYFP-Dnmt3a by mutagenesis. The presence of each desired mutation was checked by sequencing.

In Vivo Labeling with [^{32}P]Orthophosphate

U2OS cells were washed and incubated in 4 ml phosphate-free medium containing 1.2 mCi of [^{32}P] orthophosphate (Amersham) for 4 hr at 37°C with 5% CO_2. In experiments involving labeling of Myc-Dnmt3a proteins, polyethylenimine (Euromedex) was used to transfect cells with expression plasmids. The cells were then washed three times with PBS and lysed in IPH buffer (Viré et al., 2006). For immunoprecipitation, Myc (2 μg, sc 42, Santa Cruz) or human-Dnmt3a antibody (2 μg, IMG 268, Imgenex) was used. Immunocomplexes were collected, washed four times with PBS, and then resolved by SDS-PAGE (6% polyacrylamide) prior to autoradiography.

Kinase Assays

Immunoprecipitated material from transfected U2OS cells expressing Myc-Dnmt3a were incubated for 30 min at 30°C in kinase buffer with 2.5 μCi of [γ-^{32}P]-ATP or [γ-^{32}P]-GTP (Amersham). The beads were washed four times with kinase buffer and the proteins bound to them were released and resolved by SDS-PAGE (6% acrylamide) followed by autoradiography. Apigenin (40 μM, Sigma-Aldrich) and Emodin (40 μM, Sigma) were used as CK2 kinase inhibitors, and H89 (100 μM, Sigma) and staurosporine (1 μM, Sigma) were used as PKA and PKC inhibitors, respectively. In vitro kinase assays with recombinant CK2 or various Dnmt3a fragments were performed as described previously (Williams et al., 2009). Plasmid pET28a-Dnmt3a2 and the catalytic domain of pET28a-Dnmt3a have been described (Gowher and Jeltsch, 2002). Plasmids pET28a-Dnmt3a2-S386E, pET28a-Dnmt3a2-S389E, pET28a-Dnmt3a2-S386E/S389E, and pET28a-Dnmt3a2-S386A/S389A were derived from pET28a-Dnmt3a2 by mutagenesis. pGEX6P2 3a PWWP-S386A, pGEX6P2 3a PWWP-S389A, and pGEX6P2 3aPWWP-S386A/S389A were derived from pGEX6P2 3a-PWWP by site-directed mutagenesis (Dhayalan et al., 2010). The pGEX6P2 3a ADD domain constructs were prepared by cloning of the PCR product amplified from the Dnmt3a full-length construct (Zhang et al., 2010). All constructs were checked by DNA sequencing.

Mass Spectrometry

The extended PWWP domain (residues 279–420) was phosphorylated by recombinant CK2 as described above and digested with chymotrypsin. The resulting peptides were analyzed by MALDI mass spectroscopy with the help of an Autospot II device (Bruker Daltonics), as previously described (Bonk et al., 2002). At a sequence coverage of 72.4% and an intensity coverage of 38.2%, we observed one peptide (2052.96 Da) corresponding to a doubly phosphorylated fragment (FPACHDSDESDSGKAVEV, theoretical mass: 2052.73 Da) containing S386 and S389. This peak was not detected in the absence of phosphorylation and it does not correspond to any theoretical unmodified peptide from PWWP.

Antibody Generation and Western Blotting

Antibody against S390/S393-phosphorylated human Dnmt3a was raised with a keyhole limpet hemocyanin (KLH)-conjugated doubly phosphorylated peptide. The phosphopeptide-KLH conjugates were used to immunize rabbits according to standard protocols. This antibody is commercialized by Abcam (ab87763). For western blotting, U2OS cells were resuspended in SDS-PAGE buffer, sonicated, and incubated at 70°C for 15 min. The suspension was centrifuged, and the equivalent of 1 × 10^5 cells was fractionated by SDS-PAGE. After transfer, the nitrocellulose membrane was probed and reprobed with the indicated antibodies according to standard protocols. Antibodies against CK2α (polyclonal antiserum directed against the C-terminal synthetic peptide α-[376–391]) have been described (Vilk et al., 2001). Antibodies against Myc (Santa Cruz, sc42) and β-actin (Abcam, ab8226) were used for immunoprecipitation or western blotting as indicated in the figure legends.

DNA Methyltransferase Assays

His-Dnmt3a was expressed and purified and DNA methylation experiments were conducted as described previously (Jurkowska et al., 2008). Alternatively, transfected-cell extracts were used for DNA methyltransferase assays carried out as previously described (Brenner et al., 2005; Viré et al., 2006).

The transfecting plasmids have been described (Fuks et al., 2000; Penner et al., 1997). Error bars represent SD of duplicates.

Quantification of Global 5mC

Quantification of 5mC by HPCE was performed as previously described (Fraga et al., 2005). Error bars represent SD of at least two replicates. In Figure 3D, we used two inducible Tet-Off U2OS cell lines, one stably transfected with a construct encoding CK2α WT and the other with a construct encoding a catalytically inactive mutant (Vilk et al., 1999). The observed difference between the two low-CK2α controls (lane 1 versus 3) is likely due to the known impact of cell culture passages on DNA methylation levels (e.g., Shmookler Reis and Goldstein, 1982), the number of passages having been different for the two lines.

RNAi, Retroviral Infection, and RT-PCR Analysis

Interfering RNAs targeting CK2α were generated as previously described (Deplus et al., 2013). Briefly, the target sequence used to silence CK2α was inserted as a short hairpin into the pRetroSuper (pRS) retroviral vector according to the manufacturer's recommendations (OligoEngine) to form RNAi CK2α. Retrovirus production by HEK293 gag-pol cells and infection of target cells were performed as described elsewhere (Viré et al., 2006). Infected cells were selected with 1 μg/ml puromycin (Sigma). RNA purification and RT-PCR analysis were performed as described previously (Viré et al., 2006). Primer sequences are listed in Table S1.

ACCESSION NUMBERS

The Gene Expression Omnibus accession numbers for methylation data and MethylCap-seq data reported in this paper are GSE26164 and GSE26810, respectively.

SUPPLEMENTAL INFORMATION

Supplemental Information includes Supplemental Experimental Procedures, seven figures, and one table and can be found with this article online at http://dx.doi.org/10.1016/j.celrep.2014.06.048.

AUTHOR CONTRIBUTIONS

R.D., L.B., A.R., and H.B. designed experiments, performed research, and interpreted data. Experiments involving kinase-related assays were done by R.D., L.B., A.R., H.B., and J.L. Cloning, mutagenesis, and RNAi experiments were done by R.D., H.D., P.P., and E.C. R.D., L.B., J.L., and A.R. performed DNMT enzymatic assays and immunofluorescence experiments. Mass spectrometry was done by A.R. and T.P.J. HPCE assays were done by M.B. and M.F.F. Infinium methylation assays were done by S.D. and E.C. A.B. and F.S. performed MethylCap-seq experiments. M.D., F.M., C.B., and A.B. conducted bioinformatic analyses. D.W.L. provided CK2 Tet-Off cells. Y.d.L., H.G.S., and M.E. contributed to the design and interpretation of the kinase assays (Y.d.L.), MethylCap-seq (H.G.S.), and HPCE (M.E.). A.J. and F.F. designed experiments, interpreted data, and directed the study. R.D. prepared the figures. H.B., A.J., and F.F. wrote the manuscript.

ACKNOWLEDGMENTS

R.D., L.B., H.B., J.L., S.D., H.D., and E.C. were supported by the Belgian FNRS. F.F. is an FNRS "Senior Research Associate." F.F.'s lab was funded by grants from the F.N.R.S and Télévie, the "Interuniversity Attraction Poles" (IAP P6/28 and IAP P7/03), by the "Action de Recherche Concertée" (AUWB-2010-2015 ULB-No 7), and by the E.U. grant CANCERDIP FP7-200620. A.R., T.P.J., and A.J. were supported by the Deutsche Forschungsgemeinschaft (Je 252/6-1).

Received: August 30, 2013
Revised: May 6, 2014
Accepted: June 23, 2014
Published: July 24, 2014

REFERENCES

Allende, J.E., and Allende, C.C. (1995). Protein kinases. 4. Protein kinase CK2: an enzyme with multiple substrates and a puzzling regulation. FASEB J. *9*, 313–323.

Bae, J.M., Shin, S.H., Kwon, H.J., Park, S.Y., Kook, M.C., Kim, Y.W., Cho, N.Y., Kim, N., Kim, T.Y., Kim, D., and Kang, G.H. (2012). ALU and LINE-1 hypomethylations in multistep gastric carcinogenesis and their prognostic implications. Int. J. Cancer *131*, 1323–1331.

Bibikova, M., Le, J., Barnes, B., Saedinia-Melnyk, S., Zhou, L., Shen, R., and Gunderson, K.L. (2009). Genome-wide DNA methylation profiling using Infinium® assay. Epigenomics *1*, 177–200.

Brenner, C., Deplus, R., Didelot, C., Loriot, A., Viré, E., De Smet, C., Gutierrez, A., Danovi, D., Bernard, D., Boon, T., et al. (2005). Myc represses transcription through recruitment of DNA methyltransferase corepressor. EMBO J. *24*, 336–346.

Bock, C., Tomazou, E.M., Brinkman, A.B., Müller, F., Simmer, F., Gu, H., Jäger, N., Gnirke, A., Stunnenberg, H.G., and Meissner, A. (2010). Quantitative comparison of genome-wide DNA methylation mapping technologies. Nat. Biotechnol. *28*, 1106–1114.

Bonk, T., Humeny, A., Sutter, C., Gebert, J., von Knebel Doeberitz, M., and Becker, C.M. (2002). Molecular diagnosis of familial adenomatous polyposis (FAP): genotyping of adenomatous polyposis coli (APC) alleles by MALDI-TOF mass spectrometry. Clin. Biochem. *35*, 87–92.

Chen, T., Ueda, Y., Xie, S., and Li, E. (2002). A novel Dnmt3a isoform produced from an alternative promoter localizes to euchromatin and its expression correlates with active de novo methylation. J. Biol. Chem. *277*, 38746–38754.

Chen, T., Tsujimoto, N., and Li, E. (2004). The PWWP domain of Dnmt3a and Dnmt3b is required for directing DNA methylation to the major satellite repeats at pericentric heterochromatin. Mol. Cell. Biol. *24*, 9048–9058.

Cordaux, R., and Batzer, M.A. (2009). The impact of retrotransposons on human genome evolution. Nat. Rev. Genet. *10*, 691–703.

Deaton, A.M., and Bird, A. (2011). CpG islands and the regulation of transcription. Genes Dev. *25*, 1010–1022.

Denis, H., Ndlovu, M.N., and Fuks, F. (2011). Regulation of mammalian DNA methyltransferases: a route to new mechanisms. EMBO Rep. *12*, 647–656.

Deplus, R., Delatte, B., Schwinn, M.K., Defrance, M., Méndez, J., Murphy, N., Dawson, M.A., Volkmar, M., Putmans, P., Calonne, E., et al. (2013). TET2 and TET3 regulate GlcNAcylation and H3K4 methylation through OGT and SET1/COMPASS. EMBO J. *32*, 645–655, TET2 and TET3 regulate GlcNAcylation and H3K4 methylation through OGT and SET1/COMPASS.

Dhayalan, A., Rajavelu, A., Rathert, P., Tamas, R., Jurkowska, R.Z., Ragozin, S., and Jeltsch, A. (2010). The Dnmt3a PWWP domain reads histone 3 lysine 36 trimethylation and guides DNA methylation. J. Biol. Chem. *285*, 26114–26120.

Fraga, M.F., Ballestar, E., Villar-Garea, A., Boix-Chornet, M., Espada, J., Schotta, G., Bonaldi, T., Haydon, C., Ropero, S., Petrie, K., et al. (2005). Loss of acetylation at Lys16 and trimethylation at Lys20 of histone H4 is a common hallmark of human cancer. Nat. Genet. *37*, 391–400.

Fuks, F., Burgers, W.A., Brehm, A., Hughes-Davies, L., and Kouzarides, T. (2000). DNA methyltransferase Dnmt1 associates with histone deacetylase activity. Nat. Genet. *24*, 88–91.

Ge, Y.Z., Pu, M.T., Gowher, H., Wu, H.P., Ding, J.P., Jeltsch, A., and Xu, G.L. (2004). Chromatin targeting of de novo DNA methyltransferases by the PWWP domain. J. Biol. Chem. *279*, 25447–25454.

Gowher, H., and Jeltsch, A.J. (2002). Molecular enzymology of the catalytic domains of the Dnmt3a and Dnmt3b DNA methyltransferases. J. Biol. Chem. *277*, 20409–20414.

Handa, V., and Jeltsch, A. (2005). Profound flanking sequence preference of Dnmt3a and Dnmt3b mammalian DNA methyltransferases shape the human epigenome. J. Mol. Biol. *348*, 1103–1112.

Huang, J., Fan, T., Yan, Q., Zhu, H., Fox, S., Issaq, H.J., Best, L., Gangi, L., Munroe, D., and Muegge, K. (2004). Lsh, an epigenetic guardian of repetitive elements. Nucleic Acids Res. *32*, 5019–5028.

Johnson, L.N., and Barford, D. (1993). The effects of phosphorylation on the structure and function of proteins. Annu. Rev. Biophys. Biomol. Struct. *22*, 199–232.

Jurkowska, R.Z., Anspach, N., Urbanke, C., Jia, D., Reinhardt, R., Nellen, W., Cheng, X., and Jeltsch, A. (2008). Formation of nucleoprotein filaments by mammalian DNA methyltransferase Dnmt3a in complex with regulator Dnmt3L. Nucleic Acids Res. *36*, 6656–6663.

Jurkowska, R.Z., Siddique, A.N., Jurkowski, T.P., and Jeltsch, A. (2011). Approaches to enzyme and substrate design of the murine Dnmt3a DNA methyltransferase. ChemBioChem *12*, 1589–1594.

Lander, E.S. (2011). Initial impact of the sequencing of the human genome. Nature *470*, 187–197.

Law, J.A., and Jacobsen, S.E. (2010). Establishing, maintaining and modifying DNA methylation patterns in plants and animals. Nat. Rev. Genet. *11*, 204–220.

Lehnertz, B., Ueda, Y., Derijck, A.A., Braunschweig, U., Perez-Burgos, L., Kubicek, S., Chen, T., Li, E., Jenuwein, T., and Peters, A.H. (2003). Suv39h-mediated histone H3 lysine 9 methylation directs DNA methylation to major satellite repeats at pericentric heterochromatin. Curr. Biol. *13*, 1192–1200.

Lin, I.G., Han, L., Taghva, A., O'Brien, L.E., and Hsieh, C.L. (2002). Murine de novo methyltransferase Dnmt3a demonstrates strand asymmetry and site preference in the methylation of DNA in vitro. Mol. Cell. Biol. *22*, 704–723.

Lister, R., Pelizzola, M., Dowen, R.H., Hawkins, R.D., Hon, G., Tonti-Filippini, J., Nery, J.R., Lee, L., Ye, Z., Ngo, Q.M., et al. (2009). Human DNA methylomes at base resolution show widespread epigenomic differences. Nature *462*, 315–322.

Martens, J.H., Brinkman, A.B., Simmer, F., Francoijs, K.J., Nebbioso, A., Ferrara, F., Altucci, L., and Stunnenberg, H.G. (2010). PML-RARalpha/RXR Alters the Epigenetic Landscape in Acute Promyelocytic Leukemia. Cancer Cell *17*, 173–185.

Mazzorana, M., Pinna, L.A., and Battistutta, R. (2008). A structural insight into CK2 inhibition. Mol. Cell. Biochem. *316*, 57–62.

Okano, M., Bell, D.W., Haber, D.A., and Li, E. (1999). DNA methyltransferases Dnmt3a and Dnmt3b are essential for de novo methylation and mammalian development. Cell *99*, 247–257.

Penner, C.G., Wang, Z., and Litchfield, D.W. (1997). Expression and localization of epitope-tagged protein kinase CK2. J. Cell. Biochem. *64*, 525–537.

Roller, A., Grossmann, V., Bacher, U., Poetzinger, F., Weissmann, S., Nadarajah, N., Boeck, L., Kern, W., Haferlach, C., Schnittger, S., et al. (2013). Landmark analysis of DNMT3A mutations in hematological malignancies. Leukemia *27*, 1573–1578.

Rollins, R.A., Haghighi, F., Edwards, J.R., Das, R., Zhang, M.Q., Ju, J., and Bestor, T.H. (2006). Large-scale structure of genomic methylation patterns. Genome Res. *16*, 157–163.

Shmookler Reis, R.J., and Goldstein, S. (1982). Variability of DNA methylation patterns during serial passage of human diploid fibroblasts. Proc. Natl. Acad. Sci. USA *79*, 3949–3953.

St-Denis, N.A., and Litchfield, D.W. (2009). Protein kinase CK2 in health and disease: From birth to death: the role of protein kinase CK2 in the regulation of cell proliferation and survival. Cell. Mol. Life Sci. *66*, 1817–1829.

Trembley, J.H., Wang, G., Unger, G., Slaton, J., and Ahmed, K. (2009). Protein kinase CK2 in health and disease: CK2: a key player in cancer biology. Cell. Mol. Life Sci. *66*, 1858–1867.

Vilk, G., Saulnier, R.B., St Pierre, R., and Litchfield, D.W. (1999). Inducible expression of protein kinase CK2 in mammalian cells. Evidence for functional specialization of CK2 isoforms. J. Biol. Chem. *274*, 14406–14414.

Vilk, G., Derksen, D.R., and Litchfield, D.W. (2001). Inducible expression of the regulatory protein kinase CK2beta subunit: incorporation into complexes with catalytic CK2 subunits and re-examination of the effects of CK2beta on cell proliferation. J. Cell. Biochem. *84*, 84–99.

Viré, E., Brenner, C., Deplus, R., Blanchon, L., Fraga, M., Didelot, C., Morey, L., Van Eynde, A., Bernard, D., Vanderwinden, J.M., et al. (2006). The Polycomb group protein EZH2 directly controls DNA methylation. Nature *439*, 871–874.

Williams, C.C., Basu, A., El-Gharbawy, A., Carrier, L.M., Smith, C.L., and Rowan, B.G. (2009). Identification of four novel phosphorylation sites in estrogen receptor alpha: impact on receptor-dependent gene expression and phosphorylation by protein kinase CK2. BMC Biochem. *10*, 36.

Xie, H., Wang, M., Bonaldo, Mde.F., Rajaram, V., Stellpflug, W., Smith, C., Arndt, K., Goldman, S., Tomita, T., and Soares, M.B. (2010). Epigenomic analysis of Alu repeats in human ependymomas. Proc. Natl. Acad. Sci. USA *107*, 6952–6957.

Zhang, Y., Jurkowska, R., Soeroes, S., Rajavelu, A., Dhayalan, A., Bock, I., Rathert, P., Brandt, O., Reinhardt, R., Fischle, W., and Jeltsch, A. (2010). Chromatin methylation activity of Dnmt3a and Dnmt3a/3L is guided by interaction of the ADD domain with the histone H3 tail. Nucleic Acids Res. *38*, 4246–4253.